ADVANCES IN ATMOSPHERIC SCIENCES, VOL. 20, NO. 1, 2003, PP. 1–16

Amplitude-Phase Characteristics of the Annual Cycle of Surface Air Temperature in the Northern Hemisphere

Alexey V. ELISEEV * and Igor I. MOKHOV

A.M. Obukhov Institute of Atmospheric Physics RAS,
3 *Pyzhevsky*, 109017 *Moscow, Russia*

(Received December 3, 2001; revised August 12, 2002)

ABSTRACT

The amplitude phase characteristics (APC) of surface air temperature (SAT) annual cycle (AC) in the Northern Hemisphere are analyzed. From meteorological observations for the 20th century and meteorological reanalyses for its second half, it is found that over land negative correlation of SAT AC amplitude with annual mean SAT dominates. Nevertheless, some exceptions exist. The positive correlation between these two variables is found over the two desert regions: in northern Africa and in Central America. Areas of positive correlations are also found for the northern Pacific and for the tropical Indian and Pacific Oceans. Southward of the characteristic annual mean snow ice boundary (SIB) position, the shape of the SAT AC becomes more sinusoidal under climate warming. In contrast, northward of it, this shape becomes less sinusoidal. The latter is also found for the above-mentioned two desert regions. In the Far East (southward of about 50°N), the SAT AC shifts as a whole: here its spring and autumn phases occur earlier if the annual mean SAT increases. From energy-balance climate considerations, those trends for SAT AC APC in the middle and high latitudes are associated with the influence of the albedo SAT feedback due to the SIB movement. In the Far East the trends are attributed to the interannual cloudiness variability, and in the desert regions, to the influence of a further desertification and/or scattering aerosol loading into the atmosphere. In the north Pacific, the exhibited trends could only be explained as a result of the influence of the greenhouse-gases loading on atmospheric opacity. The trends for SAT AC APC related to the SIB movement are simulated reasonably well by the climate model of intermediate complexity (IAP RAS CM) in the experiment with greenhouse gases atmospheric loading. In contrast, the tendencies resulting from the cloudiness variability are not reproduced by this model. The model also partly simulates the tendencies related to the desertification processes.

Key words: annual cycle, temperature-albedo feedback, cloudiness variation, climate model

P4 4

1. Introduction

Being the most prominent climatic oscillation, the annual cycle (AC) of climate variables undergoes change under a changing climate. It is well known that the AC range (difference between summer and winter values) of surface air temperature (SAT) T_s over land mostly decreases under the currently observed global warming (Budyko and Izrael, 1987; Houghton et al., 1996; Mokhov and Eliseev, 1997; Houghton et al., 2001). This tendency is well reproduced by the state-of-the-art coupled general circulation models under increased greenhouse gases (GHG) atmospheric content (e.g., Schlesinger and Mitchell, 1986).

On the other hand, this relationship can be changed for different climate states. For instance, paleoreconstructions show that during the Late Pleistocene period, the SAT AC range was larger than the present day for both cold (glacials) and warm (e.g., the Holocene Optimum or the mid-Cretaceous Interglacial) epochs (Monin and Shishkov, 1979; Velichko, 1999; Valdes, 2000). The former case corresponds to the negative correlation between SAT AC range and annual mean SAT. In contrast, the latter case corresponds to the positive correlation between them. For the case of the Holocene Optimum, this positive correlation is usually attributed to the larger (on about 5%) interseasonal range of the top-of-the-atmosphere insolation (Valdes, 2000; Houghton et al., 2001). But even stronger relative increase of SAT AC range during the same epoch (about 10% (Valdes, 2000)), leads

*E-mail: lesha@omega.ifaran.ru

one to the hypothesis that additionally this can be due to different climatic feedbacks. During glacials, the climate was colder and drier than the present day (Monin and Shishkov, 1979) with a larger snow ice covered area. This implies a higher importance of the SAT planetary albedo (PA) feedback due to the movement of the snow–ice boundary (SIB) and diminished importance of the feedbacks associated with the atmospheric hydrological cycle. In contrast, during interglacials the warmer and wetter climate (Monin and Shishkov, 1979) implies a higher importance for the latter feedbacks, and diminished importance for the former. All this illustrates how different feedbacks may counteract the formation of the SAT AC and its sensitivity for different climate states.

Additionally, prominent changes are found in SAT AC phase characteristics (Thompson, 1995; Eliseev et al., 2000) for instrumental temperature records. These characteristics are also found to be dependent on both external forcing (e.g., solar input into the climate system or anthropogenic forcing) and climatic feedbacks.

Indices based on surface air temperature (including its annual cycle) are used to diagnose other climate characteristics, e.g., permafrost cover (Nechaev, 1981; Anisimov and Nelson, 1996). This affords one to support a direct analysis of such characteristics by a respective analysis of SAT AC.

The goal of this paper is to analyze the dynamics of the amplitude–phase characteristics of SAT AC over the Northern Hemisphere (NH) during the 20th century using the data of instrumental observations and reanalyses. Physical causes of these dynamics are analyzed based on climate models such as the energy balance model (EBM) and the global climate model of intermediate complexity developed at the A.M. Obukhov Institute of Atmospheric Physics of the Russian Academy of Sciences (IAP RAS CM) (Petoukhov et al., 1998; Handorf et al., 1999; Mokhov et al., 2002). The latter model is also used to project SAT AC changes for the 21st century. An application of these results to the diagnostics of permafrost evolution is discussed.

2. AC amplitude–phase characteristics

AC amplitude-phase characteristics are treated in terms of the conventional Fourier-analysis and of the method developed in Mokhov (1985, 1993). In the first case (Fourier-analysis), the amplitudes of annual $T_{s,1}$ and semiannual $T_{s,2}$ SAT harmonics are used as representatives of annual cycle amplitude and phase characteristics, respectively. In the second case, three variables are studied here: moments of 0- and π-phases ($t_s^{(\uparrow)}$ and $t_s^{(\downarrow)}$ respectively) and interval of exceeding $t_s^{(+)}$. The first two variables are respectively the spring and autumn moments when SAT equals to its annual mean value $T_{s,m}$. The interval of exceeding is a period between $t_s^{(\uparrow)}$ and $t_s^{(\downarrow)}$ when the local SAT is higher than its annual mean value (Mokhov, 1985, 1993).

The grounds to use amplitude of semiannual harmonics as one of the AC phase characteristics can be justified by the relations between it and other AC phase characteristics. In particular, for $T_{s,2} \ll T_{s,1}$ it can be derived

$$t_s^{(\uparrow)} = -\frac{1}{\nu_a}\left[\phi_{s,1} + \frac{T_{s,2}}{T_{s,1}}\sin(\phi_{s,2} - 2\phi_{s,1})\right], \quad (1)$$

$$t_s^{(\downarrow)} = \frac{1}{\nu_a}\left[\pi - \phi_{s,1} + \frac{T_{s,2}}{T_{s,1}}\sin(\phi_{s,2} - 2\phi_{s,1})\right], \quad (2)$$

$$t_s^{(+)} = t_s^{(\downarrow)} - t_s^{(\uparrow)} = \frac{1}{\nu_a}\left[\pi + 2\frac{T_{s,2}}{T_{s,1}}\sin(\phi_{s,2} - 2\phi_{s,1})\right], \quad (3)$$

where $\phi_{s,1}$ and $\phi_{s,2}$ are initial phases of annual and semiannual harmonics respectively, $\nu_a = 2\pi/t_a$, $t_a = 1$ yr.

If a decrease (increase) of $T_{s,2}$ is observed then one could expect a corresponding decrease (increase) of difference between $t_s^{(+)}$ and the value which equals 6 months. This can be treated as an annual cycle harmonization (deharmonization).

3. SAT AC characteristics in observations and reanalyses

3.1 *Data*

Here the following surface air temperature data are used:

- The instrumental station data (Razuvaev et al., 1992; Eischeid et al., 1991; Karl et al., 1984; Quinlan et al., 1987; Manley, 1974) for the 20th century.
- The analysis by Gruza et al. (1989) for 1891–1993 averaged over the whole Northern Hemisphere land and over Europe, Asia, and North America.
- The reanalyses provided by the National Center for Environmental Prediction/National Center for Atmospheric Research (NCEP/NCAR, 1958–1998) (Kalnay et al., 1996) and by the European Centre for Medium-Range Weather Forecasts (ERA, 1979–1993) (Gibson et al., 1997).

All these datasets are stored as monthly means. It was shown by Eliseev et al., (2000) that the data with a higher temporal resolution (e.g., daily means or 10-day means) yield the results very similar to that obtained from monthly mean series but with a lower statistical significance due to the influence of weather noise and intramonth variability.

Table 1. SAT AC amplitude–phase characteristics obtained using the data by Gruza et al. (1989) for 1891–1993. Upper line shows climatological value for Y and its standard deviation $\sigma(Y)$ (in parentheses) ($Y = T_{s,1}$, $T_{s,2}$, $t_s^{(\uparrow)}$, $t_s^{(\downarrow)}$, $t_s^{(+)}$) (the first two variables are in kelvins, the last three in days). Middle line presents regression coefficient $b(Y) = dY/dT_{s,m}$ (dimensionless for $Y = T_{s,1}$ and $T_{s,2}$ and in days per Kelvin for $Y = t_s^{(\uparrow)}$, $t_s^{(\downarrow)}$, $t_s^{(+)}$) and its standard deviation (in parentheses). Bottom line shows correlation coefficient of the above linear relationship and its statistical significance (in parentheses)

	$T_{s,1}$	$T_{s,2}$	$t_s^{(\uparrow)}$	$t_s^{(\downarrow)}$	$t_s^{(+)}$
Northern	7.0 (0.2)	0.27 (0.08)	97 (1)	283 (3)	186 (1)
Hemisphere	−0.28(±0.06)	−0.04(±0.04)	+0.1(±0.6)	−0.5(±0.6)	−0.6(±0.6)
land	-0.41 (≥99%)	-0.09	0.01	-0.08	-0.09
Europe	12.0 (0.8)	0.72 (0.36)	92 (4)	277 (5)	185 (6)
	−0.77(±0.10)	-0.14(±0.06)	−0.4(±0.6)	-2.9(±0.8)	−2.5(±0.9)
	-0.61 (≥99%)	-0.24 (≥95%)	-0.06	-0.32 (≥99%)	-0.26 (≥99%)
Asia	14.9 (0.4)	0.87 (0.33)	88 (3)	277 (2)	189 (3)
	−0.75(±0.10)	+0.01(±0.11)	−0.4(±0.8)	−0.6(±0.6)	−0.2(±0.9)
	-0.60 (≥99%)	0.01	-0.05	0.10	-0.02
North	13.6 (0.5)	0.69 (0.31)	93 (3)	281 (3)	188 (3)
America	−0.61(±0.09)	−0.06(±0.07)	−0.4(±0.7)	−1.2(±0.6)	−0.8(±0.7)
	-0.55 (≥99%)	-0.09	-0.06	-0.20 (≥95%)	-0.11

3.2 *Amplitude characteristics*

The climatological value of the SAT AC amplitude characteristics $\overline{T}_{s,1}$ (here and below overbar stands for the climatological average) is maximized in the northern parts of the continents, especially over Siberia where it amounts to about 30 K. Northern continental land areas are also distinguished by the large values of standard deviation for annual harmonics amplitude $\sigma(T_{s,1}) = 2 \div 3$ K. Patterns for $\overline{T}_{s,1}$ are very similar to each other for both studied reanalyses. In the points corresponding to the instrumental station locations, they agree well to those obtained from the station series. For interannual deviations from the ERA data, one observes smaller $\sigma(T_{s,1})$ than from the NCEP data, either due to the different spanning periods or due to the differences in the data preprocessing during the reanalyses preparation. For the analysis by Gruza et al. (1989), climatological values of $T_{s,1}$ are very robust to the particular choice of spanning period and agree with those obtained from the reanalyses. For 1881–1993 they are summarized in Table 1. In particular, the value over Europe roughly corresponds to the value 10 K given by Polonsky et al. (2000) who subjectively obtained it from the ERA data. Polonsky et al. (2000) did not include the easternmost part of Europe (eastward of 45°E) into their study and this could explain some dissimilarity between these two values. Another reason for this discrepancy could be due to the differences in the spanning periods.

The annual harmonics amplitude over NH land typically shares well-known negative correlation with $T_{s,m}$, Fig. 1. Typical values of the regression coefficient $b(T_{s,1})$ of $T_{s,1}$ on $T_{s,m}$ attain $-(0.6 \div 0.9)$ for the both studied reanalyses. Corresponding maximum (in magnitude) values over land are about $-(1.0 \div 1.2)$ and $-(1.5 \div 1.6)$ for NCEP/NCAR (1958–1998) and ERA (1979-1993), respectively. This values are in agreement with the results obtained from the station data and by Mokhov and Eliseev (1997) for the whole of Eurasia. For the NCEP/NCAR data, two statistically significant areas of the corresponding positive correlation are found: over Central America ($b(T_{s,1})$ is up to +0.6) and over the northeastern part of Africa ($b(T_{s,1})$ is up to +0.9). Positive values of $b(T_{s,1})$ are found also over the northern part of the Pacific Ocean for the both reanalyses (maximum positive regression coefficient is $+(0.3 \div 0.4)$), in agreement with Mokhov and Eliseev (1997). An additional area with statistically significant positive values $b(T_{s,1}) = +(0.2 \div 0.3)$ is located near the equator in the eastern part of the Indian Ocean and in the western Pacific.

In general, the results obtained from the NCEP/NCAR and ERA reanalyses agree among each other; the only exceptions are the above-mentioned land areas in Central America and northeastern Africa and the region in the tropical oceans. In all these cases, statistically significant positive correlations betweeen $T_{s,m}$ and $T_{s,1}$ are found only for the former dataset. This is partly due to the differences between the algorithms used to prepare the two reanalyses and partly due to the different spanning periods (1958–1998 and 1979–1993 for NCEP/NCAR and ERA, respectively). Additionally, the latter period is rather short and perhaps does not allow one to obtain statitically significant results for these two regions. One has to note, however, that the values of $b(T_{s,1})$ computed from the ERA data, while statistically insignificant, are positive over northeastern Africa but with smaller magnitudes in comparison with those computed from the NCEP/NCAR dataset. If the NCEP/NCAR reanalysis is shortened to embed only 1979–1993, the same

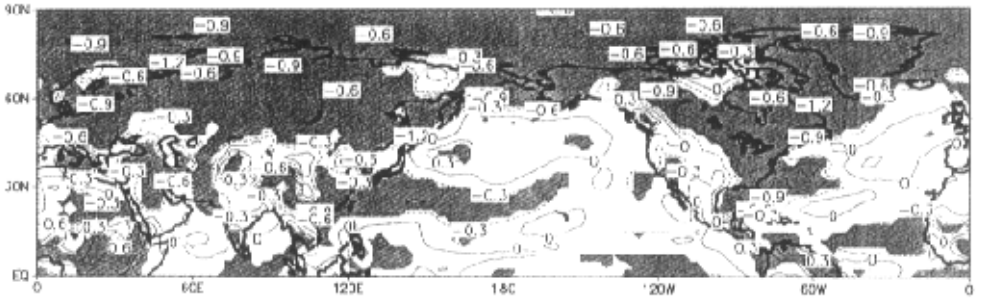

Fig. 1. Slope of the regression of amplitude of the annual harmonics on annual mean SAT obtained from the NCEP/NCAR reanalysis data for 1958–1998.

period as for the ERA data, the areas of positive correlations in northeastern Africa and in Central America still exist for the NCEP/NCAR dataset but shrink substantially. The similar area in the Indian Ocean also still exists but disappears completely in the tropical Pacific. The values obtained from the reanalyses are in agreement with the results based on the station data (not shown) and on the analysis data by Gruza et al. (1989), Table 1. Very similar results were also obtained by Mokhov and Eliseev (1997) for Eurasia and North America based on the gridded instrumental data by Jones et al. (1994).

3.3 *Phase characteristics*

The climatological pattern of SAT AC phase characteristics obtained from both the reanalyses and the station data shows that the semiannual harmonics amplitude $T_{s,2}$ is largest over the northern parts of the continents (poleward about 60°N) where it attains $2 \div 3$ K. These regions also show the largest values for standard deviations $\sigma(T_{s,2})$ of semiannual harmonics amplitude amounting to $1.5 \div 2$ K. Other regions with large values of $\overline{T}_{s,2}$ lie over the midlatitudinal western coast of North America (up to 2 K for the NCEP/NCAR dataset) and over the northern part of Africa (up to 2 K and 3 K for NCEP/NCAR and ERA data respectively). The NCEP/NCAR reanalysis also shows large values of $\overline{T}_{s,2}$ over the Arctic Ocean ($2.5 \div 4.5$ K), an important feature which is missed in the ERA data.

The spring phase moments are smaller over the continents ($90 \div 120$ days since the beginning of the year) than over the oceans ($100 \div 150$ days). The same is valid for the π-phase moment: over the continents $\overline{t_s^{(\downarrow)}} = 270 \div 290$ days, over the oceans $\overline{t_s^{(\downarrow)}} = 300 \div 310$ days. All this reflects the well-known delay of the SAT AC over ocean in comparison to that over the continents. The interval of exceeding is rather close to half of the year over most of the NH ($170 \div 185$ days) with the smallest values over the midlatitudinal Pacific (down to 150 days) and with the largest near the Labrador Peninsula (up to 200 days). The interannual standard deviations for all three variables are maximal over the continents near 65°N (up to 10 days for $t_s^{(\uparrow)}$ and $t_s^{(\downarrow)}$ and up to 14 days for $t_s^{(+)}$).

In general, the regression patterns of the SAT AC phase characteritics on the annual mean SAT shows more regional behaviour than those for amplitude characteristics. Examples of the regression coefficients for SAT AC phase characteristics are shown in Figs. 2 and 3 and in Table 1.

In the area just southward of the characteristic annual mean SIB position, the annual mean warming is accompanied by general decrease of $T_{s,2}$ and $t_s^{(+)}$ and by shifts of $t_s^{(\uparrow)}$ and $t_s^{(\downarrow)}$ to the end and to the beginning of the year respectively. Typical values of the corresponding linear regression coefficients are about $b(T_{s,2}) = -(0.2 \div 0.4)$, $b(t_s^{(\uparrow)}) = +(1 \div 6)$ day/K, $b(t_s^{(\downarrow)}) = -(2 \div 4)$ day/K, $b(t_s^{(+)}) = -(1 \div 8)$ day/K (it can be treated as a SAT AC harmonization). This corresponds to the values of interannual standard deviations for the last few decades $\sigma(T_{s,2}) = 0.6 \div 1.0$ K, $\sigma(t_s^{(+)}) = 7 \div 15$ days, $\sigma(t_s^{(\uparrow)}) = 5 \div 11$ days and $\sigma(t_s^{(\downarrow)}) = 5 \div 12$ days. In contrast, northward of the characteristic SIB position (e.g., in the region of the Siberian and Canadian Highs), $b(T_{s,2}) = +(0.1 \div 0.3)$, $b(t_s^{(\uparrow)}) = -(2 \div 3)$ day/K, $b(t_s^{(\downarrow)}) = +(0.8 \div 0.9)$ day/K, $b(t_s^{(+)}) = +(1 \div 2)$ day/K (SAT AC is deharmonized) with $\sigma(T_{s,2}) = 0.7 \div 1.5$ K, $\sigma(t_s^{(\uparrow)}) = 4 \div 12$ days.

Some peculiarities for SAT AC phase characteristics are also found for the Far East (southward of about 50°N) where the growth of $T_{s,m}$ is accompanied by shifts of both 0- and π-phase to the beginning of the year while no significant changes in interval of exceeding are found. Typically, regression coefficients

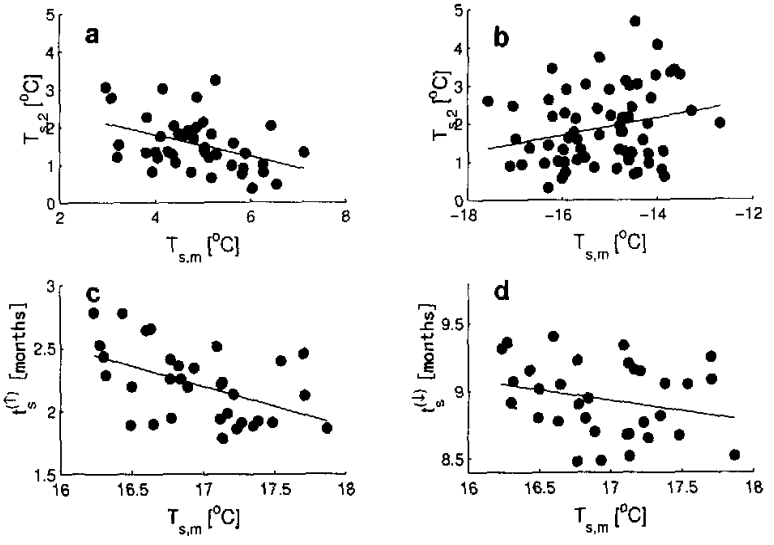

Fig. 2. Dependence of phase characteristics of SAT annual cycle on annual mean surface air temperature for the station data: (a) amplitude of the semiannual harmonics for Moscow, 56°N 38°E, 1949–1990, (b) the same but for Verkhoyansk, 67°N 134°E, 1916–1990, (c) and (d) 0- and π-phase moments respectively for Xichang, 28°N 102°E, 1950–1987.

are $b(t_s^{(\uparrow)}) = -(3 \div 6)$ day/K, $b(t_s^{(+)}) = -(10 \div 20)$ day/K, $(\sigma(t_s^{(\uparrow)}) = 3 \div 11$ days, $\sigma(t_s^{(+)}) = 12 \div 15$ days).

The desert regions in northern Africa and in Central America (including the California Peninsula) are characterized by a general deharmonization of SAT AC under a warming climate. In the former region, $b(T_{s,2}) = +(0.2 \div 0.4)$ $(\sigma(T_{s,2}) = 0.4 \div 0.6$ K), $b(t_s^{(\uparrow)}) = +(10 \div 20)$ day/K $(\sigma(t_s^{(\uparrow)}) \approx 10$ days). For the latter, $b(t_s^{(\uparrow)}) = -(10 \div 15)$ day/K $(\sigma(t_s^{(\uparrow)}) \approx 10 \div 15$ days). In both cases, $b(t_s^{(+)}) = +(10 \div 20)$ day/K $(\sigma(t_s^{(+)}) = 10 \div 20$ days).

In the stormtrack region over the northern Atlantic, one also obtains the tendency of positive correlation of 0-phase moment and annual mean SAT with $b(t_s^{(\uparrow)}) = +(3 \div 6)$ day/K and $\sigma(t_s^{(\uparrow)}) = 6 \div 10$ days. Qualitatively similar results (but in terms of annual harmonics initial phase $\phi_{s,1}$) were obtained by Thompson (1995).

4. Analysis with energy-balance climate model

In the current analysis, a Budyko-type EBM (Budyko, 1969; North and Coakley, 1979; Mokhov, 1993) is used

$$C\partial T_s/\partial t = Q(1-\alpha) - F_\uparrow - F_\rightarrow . \qquad (4)$$

Here C is the heat capacity of atmospheric-underlying surface unit column, Q the top-of-the-atmosphere incident solar radiation, α the planetary albedo, $F_\uparrow$ the outgoing longwave radiation, and $F_\rightarrow$ the meridional heat influx. Hereafter it is assumed that Q remains the same for different climate states and has no interannual and longer term variations. According to Budyko (1969),

$$F_\uparrow = (A + BT_s)\eta_c , \qquad (5)$$

where A and B are constants, and η_c is the coefficient dependent on GHG atmospheric content (η_c decreases when GHG atmospheric content increases; for the present-day climate it is convenient to take $\eta_c = 1$). Model variables can be decomposed as $Y = Y_m + Y'$ (Y stands for any model variable, and Y_m and Y' are annual mean value and seasonal variations respectively) assuming that η_c has no seasonal cycle. Hereafter ΔY stands for the summer value of Y', Y_0 for the present-day value of Y, and δY for variation of Y under climate change.

From Eqs. (4) and (5), a linearized expression for change in amplitude of the SAT annual harmonics may be derived

$$\delta T_{s,1} = -\left[B^{-1}(\Delta Q \delta\alpha_m + Q_m \delta\Delta\alpha) + T_{s,1,0}\delta\eta_c\right] , \qquad (6)$$

neglecting $\delta F_\rightarrow$.

This equation can be reduced to the sufficient conditions of $T_{s,1}$ decrease under climate warming (Mokhov and Eliseev, 1997)

$$\delta\alpha_m < 0, \qquad \delta\Delta\alpha > 0 . \qquad (7)$$

These conditions are fulfilled over the middle and high latitude land areas and explains the negative correlation between annual harmonics amplitude and annual mean SAT observed there. This effect is opposed by the decrease of atmospheric opacity for outgoing longwave radiation due to anthropogenic GHG loading into the atmosphere (see the third term on the right hand side (RHS) of Eq. (6)). Positive correlation between $T_{s,m}$ and $T_{s,1}$ in the two tropical regions (Central America and northern Africa) can be either due to desertification or due to the loading of scattering aerosol into the atmosphere. These two effects are complementary: desertification promotes higher sand dust atmospheric content. Both of them lead to the conditions

$$\delta\alpha_m > 0, \qquad \delta\Delta\alpha < 0\ , \tag{8}$$

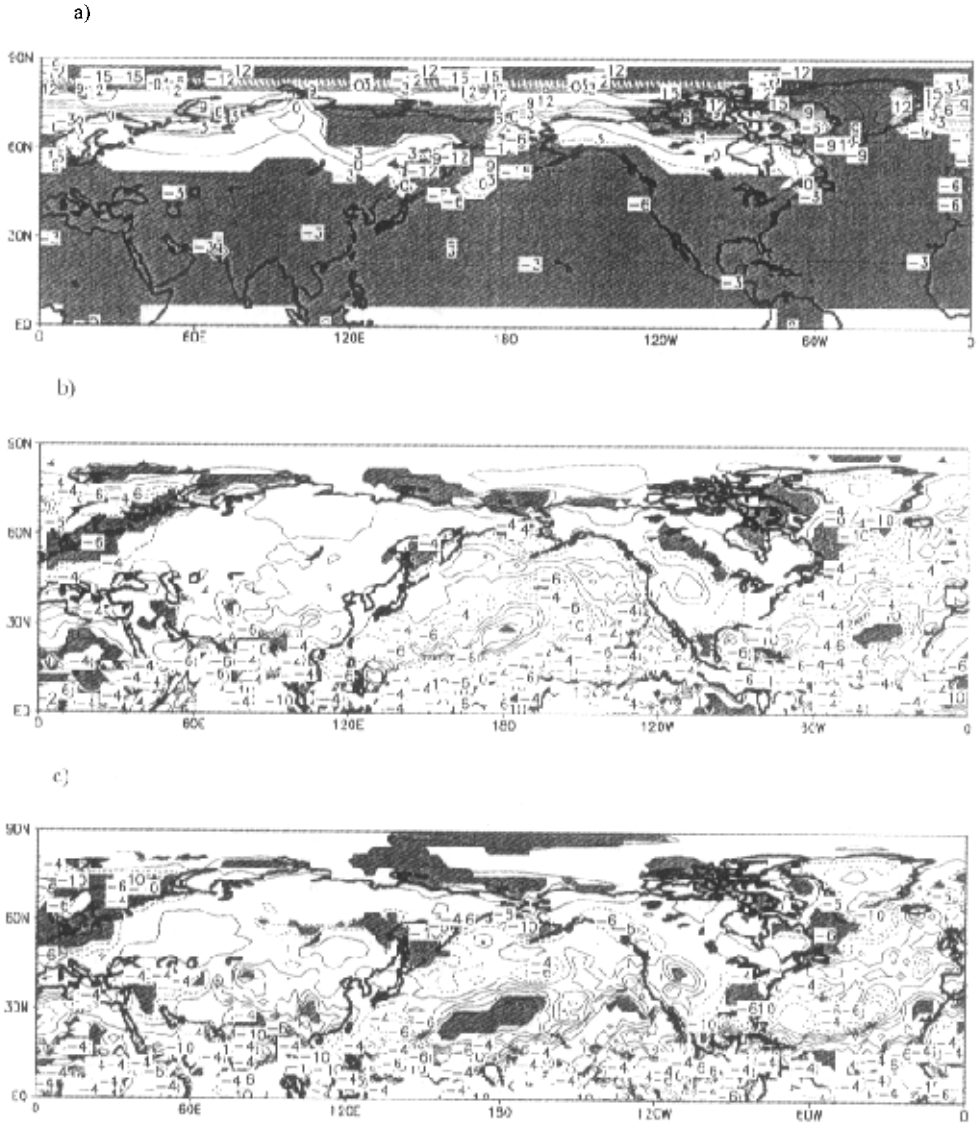

Fig. 3. Slopes of the regression for SAT AC (a) 0- and (b) π-phase moments and (c) interval of exceeding (in day/K) obtained from the NCEP/NCAR reanalysis data for 1958–1998.

which are opposite to conditions (7). Another possible contibutor to the positive correlation observed here is the above-mentioned modification of atmospheric opacity for longwave radiation due to increased GHG atmospheric content.

For phase characteristics of SAT AC it is most simple to use just 0- and π-phase moments. If their present-day values are $t_{s,0}^{(\uparrow)}$ and $t_{s,0}^{(\downarrow)}$ respectively, then taking into account the definitions of 0- and π-phases one obtains

- if $\delta t_s^{(\uparrow)} > (<)0$ then $\delta t_s^{(\uparrow)} < (>)0$ (i.e., 0 phase moments are shifted to the beginning (end) of the year),
- if $\delta T_s^{(\downarrow)} > (<)0$ then $\delta t_s^{(\downarrow)} > (<)0$.

Here, both $t_s^{(\uparrow)}$ and $t_s^{(\downarrow)}$ are counted from the beginning of the year and $\delta T^{(\vartheta)} = T'|_{t_{s,0}^{(\vartheta)}}$, $(\vartheta) = (\uparrow), (\downarrow)$.

For the present-day climate, $\delta T_s^{(\vartheta)} = 0$ by definition. In contrast, for different climates it could be different from zero because of the shifts of 0- and π phase moments. In particular, if $T_{s,2} \ll T_{s,1}$ and $|\delta T_{s,1}| \ll T_{s,1,0}$ (which is valid for the middle and high latitudes) one obtains

$$\delta t_s^{(\uparrow)} = -\frac{1}{\nu_a T_{s,1}} \delta T_s^{(\uparrow)} , \quad \delta t_s^{(\downarrow)} = +\frac{1}{\nu_a T_{s,1}} \delta T_s^{(\downarrow)} . \quad (9)$$

Again linearizing (4) and (5) around the annual mean state, neglecting $\delta F_{\leftrightarrow}$, and assuming that the solar radiation income and the longwave radiation outcome are almost balanced, one can derive

$$\delta T_s^{(\vartheta)} = -Q_m B^{-1} \left[\delta\alpha|_{t_{s,0}^{(\vartheta)}} - \delta\alpha_m \left(1 - Q^{(\vartheta)}/Q_m\right)\right] . \quad (10)$$

Here $\delta\alpha|_{t_{s,0}}^{(\vartheta)}$ stands for the value of PA change evaluated at the time $t_{s,0}^{(\vartheta)}$, $(\vartheta) = (\uparrow), (\downarrow)$. $Q^{(\vartheta)}$ is the intra annual variation of Q evaluated at the same time moments.

From Eq. (10), conditions for shifts of 0- and π-phase moments are

$$\delta t_s^{(\uparrow)} > (<)0 \quad \text{if} \quad \delta\alpha|_{t_{s,0}^{(\uparrow)}} > (<)(1 - Q^{(\uparrow)}/Q_m)\delta\alpha_m,$$

$$\delta t_s^{(\downarrow)} > (<)0 \quad \text{if} \quad \delta\alpha|_{t_{s,0}^{(\downarrow)}} < (>)(1 - Q^{(\downarrow)}/Q_m)\delta\alpha_m. \quad (11)$$

For instance, for the middle and subpolar latitudes, $\delta\alpha_m < 0$ under $\delta T_{s,m} > 0$ and $Q_m > Q^{(\uparrow)} > 0$ (Mokhov, 1993). As a result, the shift of $t_s^{(\uparrow)}$ to the end (beginning) of the year in the area lying to the south (north) of the annual mean SIB position can be treated as a result of smaller (larger) climate sensitivity of spring albedo in comparison to annual mean albedo. Analogously, the shift of $t_s^{(\downarrow)}$ to the beginning (end) of the year in the areas lying to the south (north) of the annual mean SIB position is related to smaller (larger) climate sensitivity of autumn albedo in comparison to annual mean albedo. These conclusions are supported by the similar relationship between variations of surface albedo in spring and autumn in the area to the north of the annual mean SIB position observed by Budyko et al. (1998). In these regions, PA variations are mainly determined by variations of surface albedo.

Physically, the mechanism of variations of SAT AC phase characteristics due to the SIB movement can be described as follows. For any particular region one can hypothesize two extremal climate states. If the climate state is a very cold one, then the region is covered by ice/snow throughout the year and the SAT-PA feedback is not activated (considering only the processes directly related to the SIB movement). A similar conclusion has to be made also for a very warm climate when the area is ice/snow free throughout the year. But for intermediate climate states (when the seasonal cycle of the snow-ice cover in the region is observed) this feedback is activated and serves as an amplifier of the semiannual harmonics of the solar radiation incoming at the top of the atmosphere. The change in $T_{s,2}$ is to result in the corresponding changes in $t_s^{(\uparrow)}$, $t_s^{(\downarrow)}$ and $t_s^{(+)}$ depending on sign of $\sin(\phi_{s,2} - 2\phi_{s,1})$ (see Eqs. (1)-(3)). From this point of view the regions lying to the north and to the south of the present-day annual mean SIB position can be distinguished by the relative tendencies of SIB movement. For the former regions, SIB comes nearer under global annual mean warming and its variability more strongly influences SAT AC. For the latter regions, it recedes and the influence of its variability diminishes. This mechanism is also consistent with the observed maximization of the interannual standard deviation for SAT AC phase characteristics near the present-day characteristic SIB position.

To examine an influence of the cloudiness-radiation interaction on SAT AC, one can use (Budyko, 1969; Mokhov and Petukhov, 1978)

$$F_\uparrow = [(A_1 - A_2 n) + (B_1 - B_2 n)T_s]\eta_c , \quad (12)$$

$$\alpha = \alpha_c n + (1 - n)\alpha_{cs} , \quad (13)$$

where n is the total cloud amount; A_1, A_2, B_1, and B_2 are constants; and α_c and α_{cs} the albedo of cloudy and cloudless subsystems, respectively. To consider only the direct influence of cloud amount variations, one may neglect variations of $F_{\leftrightarrow}$, α_c, and α_{cs}. Taking for simplicity $\delta n = \delta n_m$ one obtains

$$\delta T_{s,1} = k_1 \delta T_{s,m} + k_2 \delta n_m + k_3 \delta\eta_c , \quad (14)$$

for annual harmonics and

$$\delta T_s^{(\vartheta)} = \kappa_1^{(\vartheta)} \delta T_{s,m} + \kappa_2^{(\vartheta)} \delta n_m + \kappa_3^{(\vartheta)} \delta\eta_c , \quad (15)$$

for 0- and π-phase moments. Here

$$k_1 = B_2\Delta n_0/G,$$
$$k_2 = [\Delta Q(\alpha_{c,m,0} - \alpha_{cs,m,0}) + B_2 T_{s,1,0}]/G,$$
$$k_3 = T_{s,1,0} - (A_2 + B_2 T_{s,m,0})\Delta n_0/G,$$
$$\kappa_1^{(\vartheta)} = B_2 n_0^{(\vartheta)}/G,$$
$$\kappa_2^{(\vartheta)} = -Q^{(\vartheta)}(\alpha_{c,m,0} - \alpha_{cs,m,0})/G,$$
$$\kappa_3^{(\vartheta)} = (A_2 + B_2 T_{s,m,0}) n_0^{(\vartheta)}/G,$$
$$G = (B_1 - B_2 n_{m,0}) .$$

Here $n_0^{(\vartheta)}$ is the intra-annual variation of total cloud amount evaluated at the time $t_{s,0}^{(\vartheta)}$, $(\vartheta) = (\uparrow), (\downarrow)$. Coefficients k_j, $\kappa_j^{(\vartheta)}$, $j = 1, 2, 3$ have the meaning of partial derivatives of SAT AC APC on particular climatic variables. One has to emphasize that the meaning of the terms with $\delta\eta_c$ in Eqs. (14) and (15) differs from those in Eqs. (7) and (8). In the former case SAT–PA feedback due to the SIB movement is neglected but cloudiness variability is taken into account explicitly. In the latter case, in contrast, the SAT–PA feedback is taken into account but variability of cloudiness is not treated explicitly. The differences in conclusions about the importance of the terms with $\delta\eta_c$ in Eqs. (7) and (8) on one hand and Eqs. (14) and (15) on the other, are due to this difference.

Coefficients k_j, $\kappa_j^{(\vartheta)}$, $j = 1, 2, 3$ are evaluated using the observed SAT (Crutcher and Meserve, 1970) and total cloud amounts (Rossow and Schiffer, 1999), taking values $A_1 = -425.2$ W m^{-2}, $A_2 = -118.5$ W m^{-2}, $B_2 = 2.4$ W m^{-2} K^{-1}, $B_2 = 0.65$ W m^{-2} K^{-1} (Mokhov and Petukhov, 1978), $\alpha_{c,m,0} = 0.43$, $\alpha_{cs,m,0} = 0.57$ over snow/ice and $\alpha_{cs,m,0} = 0.15$ otherwise (Mokhov, 1981), annual mean SIB position at 60°N (Mokhov, 1993). The evaluated values of the coefficients $k_j (j = 1, 2, 3)$ are presented in Fig. 4. Figure 5 shows the evaluated values of $\partial t_s^{(\vartheta)}/\partial Y((\vartheta) = (\uparrow), (\downarrow); Y = T_{s,m}, n_m, \eta_c)$ obtained from $\kappa_j^{(\vartheta)} (j = 1, 2, 3)$ using Eq. (9). Additionally, it is assumed that both interannual variations of total cloud amounts and variations of η_c being of the order of a few percent per 1 K change in $T_{s,m}$. The former assumption is consistent with the typical sensitivity of total cloudiness to temperature variations obtained from observations for annual cycle (Mokhov, 1993) and interannual variability (Hanson, 1991; Norris and Leovy, 1994; Weare, 1994; Kaiser, 1998). The latter assumption is consistent with the results by Mokhov and Petukhov (1978). As a result one obtains that the first terms in the RHS of Eqs. (14) and (15) for the extratropics can be dropped. For the latter equation, additionally, the third term may be neglected. Coefficient k_2 is positive equatorward of about 60°N and negative poleward, while k_3 is positive everywhere in the NH. Consequently, the negative correlation between total cloud amount over the monsoon-related region and SAT observed in the interannual variability (Hanson, 1991; Norris and Leovy, 1994; Weare, 1994; Kaiser, 1998) (alongside with the SAT–PA feedback due to the SIB movement) contributes to the observed negative correlation between $T_{s,1}$ and $T_{s,m}$ over land. The positive correlation between them over the North Pacific is to be attributed to the variations in greenhouse gases content in the atmosphere. For Eq. (15) poleward of 60°N $\kappa_2^{(\uparrow)}$ ($\kappa_2^{(\downarrow)}$) is positive (negative). Equatorward of this latitude $\kappa_2^{(\uparrow)}$ ($\kappa_2^{(\downarrow)}$) is negative (positive). Using Eqs. (9) one sees that an increase (decrease) of annual mean cloud amount promotes the shift of both 0- and π phases to the end (beginning) of the year in middle latitudes and to its beginning (end) in high latitudes. This can be related to the influence of cloud amount variations on variations of planetary albedo and associated decrease of both spring and autumn rates of change of the solar heating. In particular, tendencies of change of SAT AC phase characteristics exhibited for the region of the East Asian monsoon can be related to the variations of annual mean cloud amount there. This conclusion is also supported by the results of the correlation analysis of SAT AC 0- and π -phase moments with the annual mean cloudiness data (Kaiser, 1998). For most stations located in the Far East, these two variables do show statistically significant (at the levels of 90% or even higher) positive correlation with annual mean cloud amounts for both interannual and interdecadal variability. The sign of the correlation is consistent with Fig. 5 where $\partial t_s^{(\uparrow)}/\partial T_{s,m} > 0$ at the latitudes southward of about 60°N. Reported values (Hanson, 1991; Norris and Leovy, 1994; Weare, 1994; Kaiser, 1998) for negative correlation between n_m and $T_{s,m}$ yield $b(t_s^{(\vartheta)})$ of the order $-(0.5 \div 1.0)$ day/K which is consistent with the results of section 3.

In the tropics, the relative importance of the semiannual harmonics is much higher than outside of them and the assumptions used to derive Eqs. (9) do not hold. As a result for the tropical region only the influence of cloudiness variations on the SAT AC amplitude characteristics is studied with the EBM (see Fig. 4). It is seen that in the tropics the main term is that with $\delta\eta_c$. It is negative under GHG loading into the atmosphere. Another term, potentially important for sufficiently large variations in total cloud amounts, is the term with δn_m. This term is clearly negative in the regions where desertification takes place. As a result, both terms do not contribute to (and even oppose) the observed positive value of $b(T_{s,1})$ in the two desert regions mentioned in section 3.2. One concludes that this positive value is due to the variations of surface albedo due to desertification and/or scattering aerosol

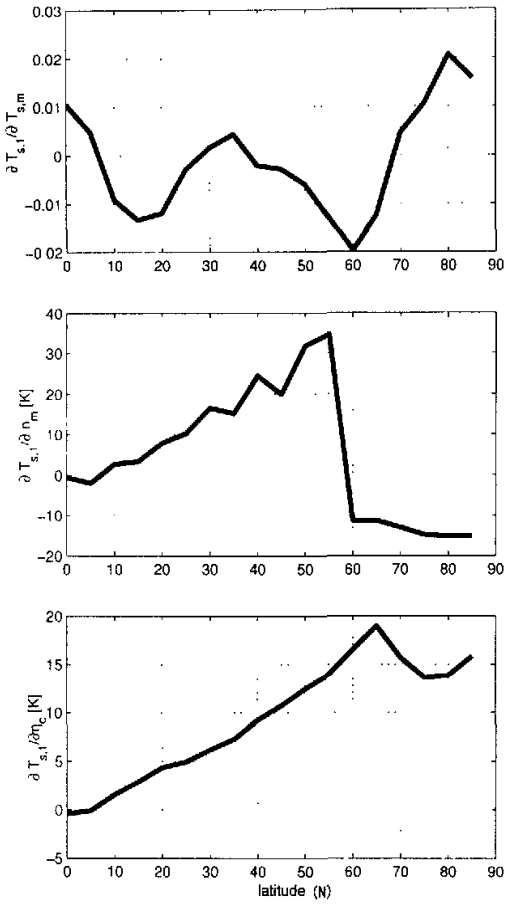

Fig. 4. Sensitivity of amplitude of the SAT annual harmonics to partial changes in (a) annual mean SAT, (b) annual mean cloud amount, and (c) GHG atmospheric content. Every sensitivity coefficient is evaluated assuming the other two variables to be constant.

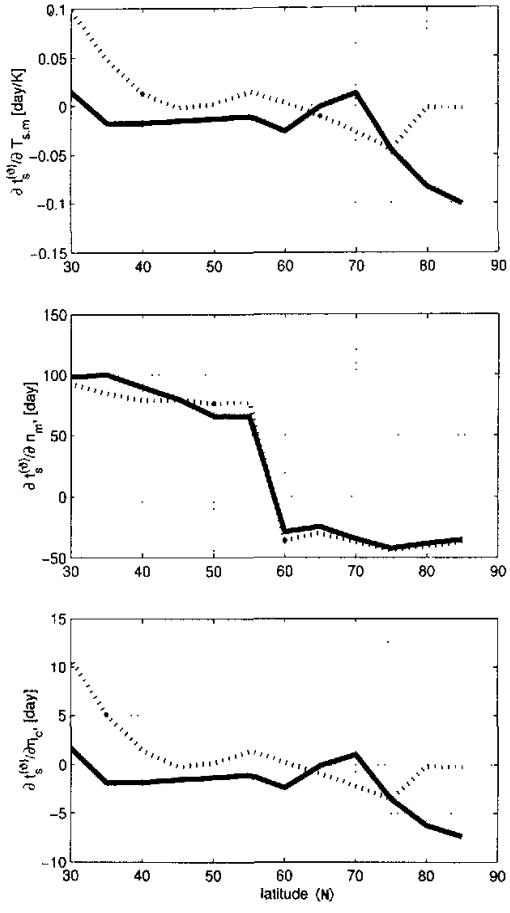

Fig. 5. Sensitivity of 0- (solid lines) and π phase (dotted lines) moments to partial changes in (a) annual mean SAT, (b) annual mean cloud amount, and (c) GHG atmospheric content. Every sensitivity coefficient is evaluated assuming the other two variables to be constant.

loading into the atmosphere.

5. Numerical experiments with IAP RAS CM

The IAP RAS CM belongs to the class of coupled atmosphere ocean-land climate models of intermediate complexity (Claussen et al., 2002). Its detailed description is given in Petoukhov et al. (1998) and Handorf et al. (1999). The run used here (Mokhov et al., 2002) was forced by the CO_2 atmospheric concentrations in accordance with the observations for 1860 1990 and with the scenario IS92a (Houghton et al., 1992) for 1991-2100. This scenario corresponds to the rise of CO_2 atmospheric content amounting to about 0.7 percent per year. The forcing due to other GHG is neglected. Globally averaged annual mean temperature increase in this run amounts to about 1.3 K to 2050 and about 2.3 K to 2100 (Mokhov et al., 2002; Demchenko et al., 2002).

5.1 *Climatological patterns*

Climatological patterns of SAT AC APC were computed for 1958-1998, the same spanning period as for the NCEP/NCAR reanalysis.

The IAP RAS CM correctly reproduces the large scale features of the patterns for $T_{s,1}$. For phase characteristics, the model's behaviour is more complex. The IAP RAS CM successively reproduces most large

scale features for $T_{s,2}$ but underestimates its value near the North Pole as it was for the ERA data. For the spring phase moment, the model yields generally correct climatological values over land but fails to reproduce its extrema over the Pacific and near the Labrador Peninsula (see section 3.3). A very similar conclusion can be made for π-phase moments and the interval of exceeding: the IAP RAS CM again correctly simulates their values over land but performs poorly over the oceans.

The model correctly simulates interannual standard deviations for SAT AC APC in the regions where they are supposed to be forced by the SIB movement (see section 4). At the same time it poorly reproduces them in the regions of high cloudiness variability (southeastern Asia, stormtracks) and in the desert regions.

5.2 *Sensitivity to climate variations*

Sensitivity to climate variations is computed in a way similar to that used for observations by performing corresponding linear regressions for selected spanning periods. In particular, the chosen periods are 1958–1998 (the same as for the NCEP/NCAR dataset), 1991–2041, and 2051–2100.

For amplitude characteristics of SAT AC, it is seen that the model correctly simulates the tendencies of change related to the SAT PA feedback due to the SIB movement, see Fig. 6 for 1991–2041 as an example. The only caveat found here is the overestimated regression coefficients over the Arctic Ocean. In contrast, the regions of positive correlation between $T_{s,t}$ and $T_{s,m}$ in the northern Pacific and northern Africa are not reproduced. In Central America there is a region of the positive correlation between these two variables for 2041–2100 but the correlation is statistically insignificant and the coefficient $b(T_{s,1})$ is small. This area of positive correlation completely disappears for 2051–2100.

A similar conclusion can be obtained for the phase characteristics of SAT AC (see Fig. 7 for 2051–2100 as an example). The IAP RAS CM simulates the as an example). The IAP RAS CM simulates the tendencies related to the feedback between SAT and planetary albedo due to the SIB movement. In particular, in Fig. 7 one clearly sees the regions of positive (negative) $b(T_{s,2})$ and $b(t_s^{(+)})$ just poleward (equatorward) of the annual mean SIB position with correct magnitudes. A similar conclusion can be made for the π–phase moment, but in this case the magnitudes for $b(t_s^{(\downarrow)})$ are overestimated. For the spring phase moment the model simulates only statistically insignificant tendencies of change. During the earlier period 1991–2041 the areas of statistically significant relationships are smaller. This is due to the smaller magnitude of change of CO_2 atmospheric content during this period in comparison to that during 2051–2100. Nevertheless, in the regions which share high statistical significance during both periods, the patterns are generally the same.

In contrast, the relationships associated with the cloudiness variability are not reproduced correctly. The model misses the relationships found for the region in the Far East and for the region of stormtracks, see section 3.3. The relationships found for $T_{s,2}$ and $t_s^{(+)}$ in the deserts in Africa and America are also generally missed, but the model yields correct magnitudes for $t_s^{(\uparrow)}$ and $t_s^{(\downarrow)}$ in these regions.

6. Discussion and conclusions

The amplitude-phase characteristics of the SAT annual cycle in the Northern Hemisphere are analyzed using meteorological observations for the 20th century and meteorological reanalyses for its second half. For amplitude characteristics (annual harmonics amplitude $T_{s,1}$), the well-known negative correlation with annual mean SAT $T_{s,m}$ is exhibited over most land

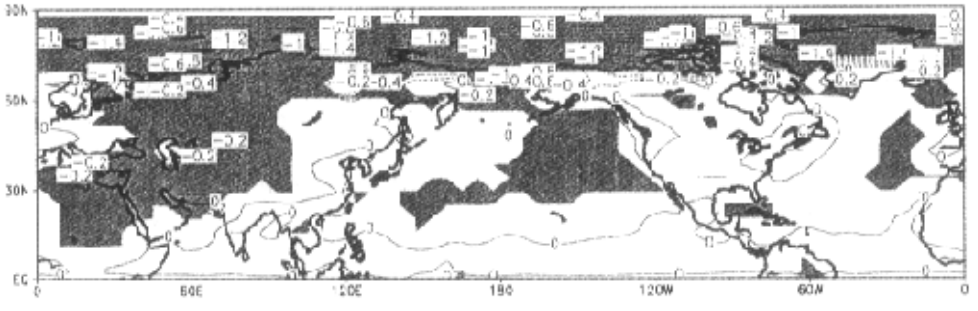

Fig. 6. Slope of the regression of amplitude of the annual harmonics on annual mean SAT obtained from the numerical experiment with the IAP RAS CM for 1991–2040.

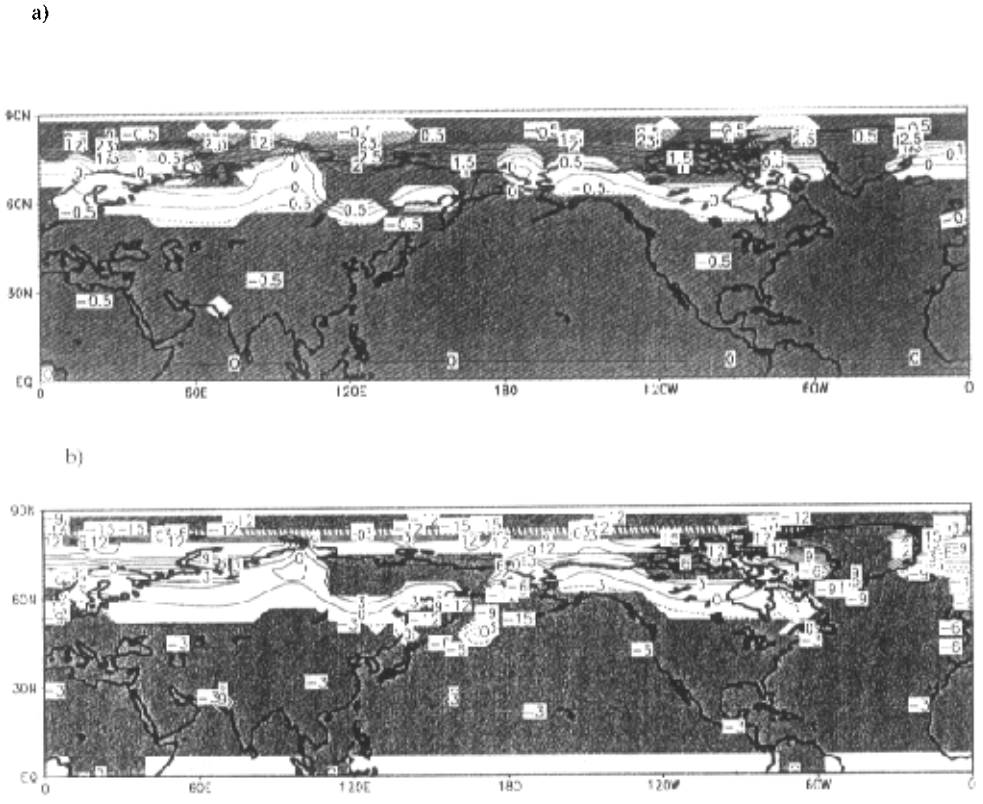

Fig. 7. Slopes of the regression of SAT AC phase characteristics on annual mean SAT obtained from the numerical experiment with the IAP RAS CM for 2051–2100. Panels: (a) amplitude of the semiannual harmonics (dimensionless), (b) interval of exceeding (in d K^{-1}).

areas. Nevertheless, some exceptions exist. In particular, these variables are positively intercorrelated over the two desert regions: in northern Africa and in Central America (the latter only for the NCEP/NCAR reanalysis data). Additionally, similar areas of positive correlations are found for the northern Pacific and for the tropical Indian and Pacific Oceans (the last two regions are again only for the NCEP/NCAR dataset).

One may note that the above-mentioned region in the two tropical oceans is a key region for the development of El Niño–Southern Oscillation (ENSO) events. The annual cycle of SAT is very important in regulating the development of tropical convection which contributes to the ENSO phenomenon (Philander and Rasmusson, 1985; Meehl, 1987; Diaz and Kiladis, 1992).

An analysis of the energy-balance climate model allows one to associate the dominating negative correlation with the SAT–PA feedback due to the SIB movement. Over northern Africa and Central America, the positive intercorrelation may be attributed to the desertification and/or scattering aerosol loading into the atmosphere. Similar positive intercorrelation over the north Pacific in the EBM could only be explained as a result of the atmospheric opacity decrease due to the greenhouse gases loading.

The SAT AC phase characteristics (semiannual harmonics amplitude $T_{s,2}$, moments of 0- and π-phases $t_s^{(\uparrow)}$ and $t_s^{(\downarrow)}$ respectively and interval of exceeding $t_s^{(+)}$) also show regional peculiarities. In particular, their interannual deviations are maximized near the characteristic position of the snow–ice boundary. Southward of the characteristic SIB annual mean position, the SAT AC is harmonized under climate warming. It is manifested by the negative correlation for amplitude of the semiannual harmonics, the moment of SAT AC π-phase and interval of exceeding with annual mean SAT and positive correlation for 0-phase moment. This is also found for the whole Europe and North America. In contrast, northward of the charac-

teristic SIB position, the SAT AC is deharmonized under climate warming and the correlation for the above mentioned phase characteristics and annual mean SAT is reversed. A similar SAT AC deharmonization is also found for the two desert regions: in northern Africa and in Central America. In the Far East (southward from about 50°N) the SAT AC shifts as a whole with its spring and autumn phases occurring earlier; both SAT AC 0- and π-phase moments are negatively correlated with the annual mean SAT while no significant changes of interval of exceeding are found.

Near the SIB annual mean position the tendencies for SAT AC phase characteristics have to be attributed to the SAT–PA feedback due to the SIB movement. In the Far East those trends may be associated with the cloudiness variability.

In the region influenced by stormtracks, however, the reported correlation (Hanson, 1991; Norris and Leovy, 1994; Weare, 1994) between cloud amounts and SAT has the same sign as in the Far East, but the tendencies for the autumn phase are statistically insignificant and for the spring phase are opposite to those obtained for the latter region. This can be treated as a result of the concurrence between the two opposing feedbacks: the SAT–PA feedback due to the SIB movement and the cloudiness feedback. The results force one to suppose that the former dominates, but this needs more detailed analysis than found in the present study to make a clear conclusion.

The IAP RAS climate model correctly reproduces the present-day patterns for SAT AC APC over land but poorly performs over the ocean. Additionally, it simulates the part of their variability which is associated with the SAT–PA feedback due to the SIB movement.

Under anthropogenic climate forcing, the IAP RAS CM correctly reproduces tendencies of change in the regions where they are supposed to be forced by the SAT–PA feedback due to the SIB movement. There is evidence that this feedback is overestimated by the model. On the other hand, the IAP RAS CM underestimates those tendencies to be associated with cloudiness variability. In the regions where a desertification is observed, the model simulates the tendencies only partly: the regression coefficients for SAT AC APC on annual mean SAT are either positive or negative depending on the selected time period.

The model shortcomings in simulating the cloudiness variability may be traced to the model representation of the dynamical processes which are highly parameterized (Petoukhov et al., 1998; Handorf et al., 1999). This leads to the limitations of the simulation of atmospheric dynamics by IAP RAS CM (at least by its current version) and, in turn, to the underestimation of the interannual variability by the model. Underestimation of the cloudiness variability also may be one of the possible reasons for the overestimation of the SAT–PA feedback related to the SIB movement. This is consistent with the generally smoothing role of the cloud cover in the PA variations between ice/snow covered and ice/snow free regions.

On the other hand, one may easily argue that the variability of the dynamical energy fluxes can be important for SAT AC APC. In the present analysis, atmospheric synoptic scale dynamics are not only parameterized in the analysis with the IAP RAS CM but also completely missed in the analysis with the energy-balance climate model. This topic needs more detailed models than those used here and is currently postponed for future work.

As was mentioned above, in the desert regions the tendencies of change for SAT AC APC may be associated either with further desertification or with scattering aerosol loading into the atmosphere. The IAP RAS CM includes the module (based on the BATS scheme (Dickinson et al., 1986)) for climate–vegetation interactions which are responsible for the former phenomenon. In contrast, the forcing due to scattering aerosol is neglected in the model: currently the IAP RAS CM treats only spatially homogeneous and time independent atmospheric aerosol. Partial reproduction of SAT AC APC tendencies of change in those regions by the model can be considered as a hint on the role of desertification. Currently it is unclear whether the misreproduced part of these tendencies is due to the omission of aerosol forcing or due to the mistreated climate vegetation feedbacks. To answer this question one needs to perform a simulation with a realistic aerosol forcing, a work which is in progress.

Also as mentioned in the introduction, the results obtained here can be used to study other climate processes. This can be done by using respective diagnostical indices which take into account SAT AC APC. In particular, the correlation between annual mean SAT and amplitude of SAT AC characteristics may be used to study the permafrost cover dynamics based on such indices (Nechaev, 1981; Anisimov and Nelson, 1996). Namely, as in the permafrost covered regions, SAT AC is very close to a pure sine-wave-shaped function, all such indices can be computed as a function of two governing parameters: $T_{\mathrm{s,m}} - T_f$ ($T_f = 0$°C is the freezing temperature of fresh water) and $T_{\mathrm{s,1}}$. These two parameters can be combined into the single dimensionless parameter $\xi = (T_{\mathrm{s,m}} - T_f)/T_{\mathrm{s,1}}$. In such a case, the temperature sensitivity for any index I can be expressed as

$$\frac{dI}{dT_{\mathrm{s,m}}} = \frac{1}{T_{\mathrm{s,1}}} \frac{dI}{d\xi} \left(1 - \xi \frac{dT_{\mathrm{s,1}}}{dT_{\mathrm{s,m}}} \right) , \qquad (16)$$

and all the information about the particular type of the index is stored in the term $dI/d\xi$. Since permafrost is formed only if $T_{\mathrm{s,m}} \leq T_f$, it is seen that

negative $dT_{s,1}/dT_{s,m}$ opposes permafrost degradation under annual mean warming and its formation under annual mean cooling. For the relative severity index (Nechaev, 1981) $I_{rs} = T_{s,min}/T_{s,max}$, where $T_{s,min}$ and $T_{s,max}$ are minimum and maximum values of SAT during the annual cycle, the continuous subsurface permafrost boundary corresponds to $I_{rs} = -2$ leading to $\xi = -1/3$. Typically, here $b(T_{s,1}) = -(0.6 \div 0.8)$ and the value in brackets in Eq. 16 deviates from unity by about $20 \div 30\%$. Positive correlation between $T_{s,m}$ and $T_{s,1}$ during climatic optima is consistent with higher temperature sensitivity of continuous permafrost cover than currently observed and modelled under anthropogenic climate forcing (Demchenko et al., 2002). Very similar results can be obtained for the surface frost index (Anisimov and Nelson, 1996). This is in contrast to the permafrost cover indices based only on annual mean SAT (Gavrilova, 1981) which temperature sensitivity is rather different from that for indices which take into account SAT AC.

Acknowledgments. The authors are indebted to V. N. Razuvaev for providing the observed surface air temperatures as well as to the personnel of the European Center for Medium-Range Weather Forecasts and National Center for Environmental Prediction/National Center for Atmospheric Research for providing the public domain reanalyses data. Useful discussions with P. F. Demchenko, V. P. Nechaev, V. K. Petoukhov, and K. G. Rubinstein are greatly acknowledged. The comments of the anonymous referee helped the authors to improve the manuscript. Station data calculations presented in the paper are done together with N. Yu. Vakalyuk. Maps are produced using the GrADS software developed at the Center for Land–Ocean Atmosphere Studies. This work has been supported by the Russian Foundation for Basic Research (Grants 02-05 64573, 00 05-64606 and 00-15-48498) and by the Russian Ministry for Industry, Science and Technology (Contracts 801-7(00)-P and 801-8(00)-P). Part of this paper has been presented at the VIII International Symposium "Atmospheric and Ocean Optics. Atmospheric Physics" (Irkutsk, 2001).

APPENDIX A

List of Abbreviations

AC	annual cycle
APC	amplitude–phase characteristics
EBM	energy–balance climate model
ERA	Reanalysis provided by the European Centre for Medium-Range Weather Forecasts
GHG	greenhouse gases
IAP RAS CM	climate model developed at the A.M. Obukhov Institute of Atmospheric Physics of the Russian Academy of Sciences
NCEP/NCAR	National Center for Environmental Prediction/National Center for Atmospheric Research
NH	Northern Hemisphere
PA	planetary albedo
RHS	right hand side
SAT	surface air temperature
SIB	snow ice boundary

APPENDIX B

List of mathematical symbols

If a variable is used only near the point where it is explained, it is not listed here.

A, B, A_1, A_2, B_1, B_2	constants of the dependence of outgoing longwave radiation on surface air temperature and cloud amount (see Eqs. (5), (12))
$b(Y)$	slope of the linear regression of a given variable Y and annual mean SAT
C	heat capacity of unit atmosphere–surface column
$F_\uparrow$	outgoing longwave radiation
$F_{\leftrightarrow}$	meridional heat influx
n	total cloud amount
$n_{m,0}$	the present-day value for annually averaged total cloud amount
Q	top-of-the-atmosphere incident solar radiation
Q_m	annual mean value of Q
$Q^{(\uparrow)}, Q^{(\downarrow)}$	deviations of Q from its annual mean value at the moments $t_{s,0}^{(\uparrow)}$ and $t_{s,0}^{(\downarrow)}$, respectively
T_s	surface air temperature
$T_{s,m}$	annual mean surface air temperature
$T_{s,m,0}$	the present-day value for annual mean surface air temperature
T_s'	intra-annual variation of T_s
$T_s^{(\uparrow)}, T_s^{(\downarrow)}$	value of T_s' evaluated at the present-day values of 0- and π-phase moments respectively (for the present-day climate it is always $t_s^{(\uparrow)}, T_s^{(\downarrow)} = 0$, for other climate states it could differ from zero)
$T_{s,1}$	amplitude of the SAT annual harmonics
$\overline{T_{s,1}}$	the climatological value for $T_{s,1}$
$T_{s,1,0}$	the present-day value of $T_{s,1}$
$T_{s,2}$	amplitude of the SAT semi-annual harmonics

$\overline{T_{s,2}}$	the climatological value for $T_{s,2}$
$t_s^{(\uparrow)}$	moment of 0 phase for SAT AC: the moment when $T_s = T_{s,m}$ in spring
$t_{s,0}^{(\uparrow)}$	the present-day value for $t_s^{(\uparrow)}$
$t_s^{(\downarrow)}$	moment of π-phase for SAT AC: the moment when $T_s = T_{s,m}$ in autumn
$\overline{t_s^{(\downarrow)}}$	the climatological value for $t_s^{(\downarrow)}$
$t_{s,0}^{(\downarrow)}$	the present-day value for $t_s^{(\downarrow)}$
$t_s^{(+)}$	interval of exceeding: the time interval between $t_s^{(\uparrow)}$ and $t_s^{(\downarrow)}$ within the same year
α	planetary albedo
α_c	cloudy planetary albedo
$\alpha_{c,m,0}$	the present-day value for annually averaged cloudy planetary albedo
α_{cs}	clear sky planetary albedo
$\alpha_{cs,m,0}$	the present-day value for annually averaged clear sky planetary albedo
ΔQ	summer deviation of Q from its annual mean value
Δn_0	the present day value for summer intra-annual variation of total cloud amount
$\delta F_{\leftrightarrow}$	change of $F_{\leftrightarrow}$ corresponding to a given climatic change
δn_m	change in the annually averaged total cloud amount corresponding to a given climatic change
$\delta\alpha_m$	change of the annual mean PA corresponding to a given climatic change
$\delta\Delta\alpha$	change of the summer intra-annual deviation of PA corresponding to a given climatic change
$\delta T_s^{(\uparrow)}, \delta T_s^{(\downarrow)}$	changes of $T_s^{(\uparrow)}$ and $T_s^{(\downarrow)}$ corresponding to a given climatic change, respectively
$\delta T_{s,1}$	change of $T_{s,1}$ corresponding to a given climatic change
$\delta t_s^{(\uparrow)}, \delta t_s^{(\downarrow)}$	changes of $t_s^{(\uparrow)}$ and $t_s^{(\downarrow)}$ corresponding to a given climatic change, respectively
$\delta\alpha\|_{t_{s,0}^{(\uparrow)}}, \delta\alpha\|_{t_{s,0}^{(\downarrow)}}$	change of PA corresponding to a given climatic change evaluated at the present-day 0- or π-phase moment, respectively
$\delta\eta_c$	change of η_c corresponding to a given climatic change
η_c	correction factor for outgoing long-wave radiation to account for its direct dependence on GHG atmospheric content
(ϑ) (superscript)	a dummy substitute either for the superscript $(\uparrow)$ or for the superscript $(\downarrow)$
ν_a	$= 2\pi/t_a$, $t_a = 1$ yr
$\sigma(Y)$	interannual standard deviation for a given variable Y
ϕ_s, j	initial phases of the SAT AC harmonics: annual if $j = 1$ and semi-annual if $j = 2$

REFERENCES

Anisimov, O. A., and F. E. Nelson, 1996: Permafrost distribution in the Northern Hemisphere under scenarios of climatic change. *Global Planet. Change*, **14**, 59–72.

Budyko, M. I., 1969: The effect of solar radiation variations on the climate of the earth. *Tellus*, **21**, 611–619.

Budyko, M. I., I. M. Baikova, N. A. Efimova, and L. A. Strokina, 1998: A relationship between surface albedo and climate change. *Rus. Meteor. Hydrol.*, (6), 1–5.

Budyko, M. I., and Yu. A. Izrael, editors, 1987: *Anthropogenic Climate Changes*. Gidrometeoizdat, Leningrad, 406 pp. (in Russian)

Claussen, M., and coauthors, 2002: Earth system models of intermediate complexity: closing the gap in the spectrum of climate system models. *Climate Dyn.*, **18**(7), 579 586.

Crutcher, H. L., and J. M. Meserve, 1970: Selected-level heights, temperatures and dew point temperatures for the Northern Hemisphere. Technical Report NAVAIR Rep. 50 1C-52, Naval Weather Service, Washington., D. C.

Demchenko, P. F., A. A. Velichko, A. V. Eliseev, I. I. Mokhov, and V. P. Nechaev, 2002: Dependence of permafrost conditions on global warming: Comparison of models, scenarios, and paleoclimatic reconstructions. *Izv. Atmos. Oceanic Phys.*, **38**(2), 143 151.

Diaz, H. F., and G. N. Kiladis, 1992: Atmospheric teleconnections associated with the extreme phase of the Southern Oscillation. *El Niño: Historical and Paleoclimatic Aspects of the Southern Oscillation*, H. F. Diaz and V. Markgraf Eds., Cambridge University Press, Cambridge, 7–28.

Dickinson, R. E., A. Henderson-Sellers, P. J. Kennedy, and M. F. Wilson, 1986: Biosphere–atmosphere transfer scheme (BATS). Technical Report NCAR/TN-275-STR, Naval Weather Service, Boulder, Colorado.

Eischeid, J. K., H. F. Diaz, R. S. Bradley, and P. D. Jones, 1991: A comprehensive precipitation data set for global land areas. Technical Report DOE/ER-69017T-H1, Carbon Dioxide Research Division, U.S. Department of Energy, Washington, D.C.

Eliseev, A. V., I. I. Mokhov, and N.Yu Vakalyuk, 2000: Tendencies of changes in the phase characteristics of the annual cycle of surface air temperature for the Northern Hemisphere. *Izv., Atmos. Oceanic Phys.*, **36**(1), 11–20.

Gavrilova, M. K., 1981: *Present Day Climate and Permafrost over Continents*. Nauka Publ. House, Novosibirsk, 112 pp. (in Russian)

Gibson, R., P. Kallberg, S. Uppala, A. Hernandez, A. Nomura, and E. Serrano, 1997: ERA description, ECMWF re-analysis project report series, Vol. 1. Technical report, European Centre for Medium-Range Weather Forecasts, Reading.

Gruza, G. V., E. Ya. Ran'kova, and Rocheva E. V., 1989: Analysis of global data on variations of surface air temperature during instrument observation period. *Soviet Meteor. Hydrol.*, (1), 16–24.

Handorf, D., V. K. Petoukhov, K. Dethloff, A. V. Eliseev, A. Weisheimer, and I. I. Mokhov, 1999: Decadal climate variability in a coupled atmosphere-ocean climate model of moderate complexity. *J. Geophys. Res.*, **104**(D22), 27253-27275.

Hanson, H. P., 1991: Marine stratocumulus climatologies. *Int. J. Climatol.*, **11**, 147–164.

Houghton, J. T., B. A. Callander, and S. K. Varney, editors, 1992: *Climate Change: The Supplementary Report to the IPCC Scientific Assessment, Intergovernmental Panel on Climate Change.* Cambridge University Press, Cambridge, 198 pp.

Houghton, J. T., Y. Ding, D. J. Griggs, M. Noguer, P. J. van der Linden, X. Dai, K. Maskell, and C. A. Johnson, editors, 2001: *Climate Change 2001: The Scientific Basis. Contribution of Working Group I to the Third Assessment Report of the Intergovernmental Panel on Climate Change.* Cambridge University Press, Cambridge/New York, 881 pp.

Houghton, J. T., L. G. Meira Filho, B. A. Callander, N. Harris, A. Kattenberg, and K. Maskell, editors, 1996: *Climate Change: The Science of Climate Change, Intergovernmental Panel on Climate Change.* Cambridge University Press, Cambridge, 572 pp.

Jones, P. D., T. M. L. Wigley, and K. R. Briffa, 1994: Global and hemispheric temperature anomalies — land and marine instrumental records. *Trends'93: A Compendium of Data on Global Change*, Kaiser, R.J. Sepanski, and F.W. Stoss, Eds., number ORNL/CDIAC-65, Carbon Dioxide Information Analysis Center, Oak Ridge National Laboratory, Oak Ridge, Tenn., 603–608.

Kaiser, D. P., 1998: Analysis of total cloud amount over China. *Geophys. Res. Lett.*, **25**(19), 3599–3602.

Kalnay, E., and Coauthors, 1996: The NCEP/NCAR 40-year reanalysis project. *Bull. Amer. Meteor. Soc.*, **77**, 437–471.

Karl, T. R., G. Kukla, and J. Gavin, 1984: Decreasing diurnal temperature range in the United States and Canada from 1941 through 1980. *J. Climate Appl. Meteor.*, **23** (11), 1489–1504.

Manley, G., 1974: Central England temperature: Monthly means 1659 to 1973. *Quart. J. Roy. Meteor. Soc.*, **100**, 389-405.

Meehl, G. A., 1987: The annual cycle and interannual variability in the tropical Pacific and Indian Ocean regions. *Mon. Wea. Rev.*, **115**(1), 27–50.

Mokhov, I. I., 1981: Effect of CO_2 on the thermal regime of the Earth's climatic system. *Soviet Meteor. Hydrol.*, (1), 17 26.

Mokhov, I. I., 1985: Method of amplitude–phase characteristics for analyzing climate dynamics. *Soviet Meteor. Hydrol.*, (5), 14–23.

Mokhov, I. I., 1993: *Diagnostics of Climate System Structure.* Gidrometeoizdat, St. Petersburg, 271 pp. (in Russian)

Mokhov, I. I., P. F. Demchenko, A. V. Eliseev, V. Ch. Khon, and D. V. Khvorostyanov, 2002: Estimation of global and regional changes in XIX XXI centuries based on the IAP RAS climate model taking into account anthropogenic influence. *Izv. Atmos. Ocean. Phys.*, **38** (5), 555 568.

Mokhov, I. I., and A. V Eliseev, 1997: Tropospheric and stratospheric temperature annual cycle: Tendencies of change. *Izv. Atmos. Oceanic Phys.*, **33**(4), 415–426.

Mokhov, I. I., and V. K. Petukhov, 1978: Parameterization of outgoing longwave radiation for climate models. Technical report, Institute of Atmospheric Physics, USSR Academy of Sciences, Moscow. (in Russian)

Monin, A. S.. and Yu. A. Shishkov, 1979: *The History of Climate.* Gidrometeoizdat, Leningrad, 408 pp. (in Russian)

Nechaev, V. P., 1981: On some relations between parameters of permafrost and their paleogeographic application. *Problems of Pleistocene Paleogeography in Glacial and Periglacial Regions*, A. A. Velichko and V. P. Grichuk, Eds., Publ. House "Nauka", Moscow, 211–220. (in Russian)

Norris, J. R., and C. B. Leovy, 1994: Interannual variability in stratiform cloudiness and sea surface temperature. *J. Climate*, **7**(12), 1915 1925.

North, G. R., and J. A. Coakley, 1979: Differences between seasonal and mean annual energy balance model calculations of climate and climate sensitivity. *J. Atmos. Sci.*, **36**(7), 1189–1204.

Petoukhov, V. K., I. I. Mokhov, A. V. Eliseev, and V. A. Semenov, 1998: *The IAP RAS Global Climate Model.* Dialogue–MSU, Moscow.

Philander, S. G., and E. M. Rasmusson, 1985: The Southern Oscillation and El Niño. *Adv. Geophys.*, **28A**, 197–215.

Polonsky, A. B., D. V. Basharin, and E. N. Voskresenskaya 2000: On oceanic influence on temperature variability of European and Mediterranean regions. *Morskoi Gidrofiz. Zhur.*, (5), 32–46. (in Russian)

Quinlan, F. T., T. R. Karl, and C. N. Williams, 1987: United States Historical Climatology Network (HCN) serial temperature and precipitation data. Technical Report NDP–019, Carbon Dioxide Information Analysis Center, Oak Ridge National Laboratory, Oak Ridge.

Razuvaev, V. N., E. G. Apasova, and R. A. Martuganov, 1992: Daily and extreme temperature data sets within the USSR. *Int. Temperature Workshop*, D. Parder, Ed., Bracknell, Hadley Centre, United Kingdom Meteorological Office.

Rossow, W. B., and R. A. Schiffer, 1999: Advances in understanding clouds from ISCCP. *Bull. Amer. Meteor. Soc.*, **80**(11), 2261-2287.

Schlesinger, M. E., and J. F. B. Mitchell, 1986: Model projections of the equilibrium climatic response to increased carbon dioxide. *Projecting the Climatic Effects of Increasing Carbon Dioxide*, M.C. MacCracken and F.M. Luther, Eds., United States Department of Energy, Washington, D.C., 81–147.

Thompson, D. J., 1995: The seasons, global temperature, and precession. *Science*, **268**, 59 68.

Valdes, P., 2000: Paleoclimate modeling. *Numerical Modeling of the Global Atmosphere in the Climate System*, P. Mote and A. O'Neill, Eds., Kluwer Acad. Publ., Dordrecht/Boston/London, 465 488.

Velichko, A. A., editor, 1999: *Climate and Environment Changes during the Last 65 Million Years(Cenozoic: from Paleocene to Holocene)*. GEOS, Moscow, 260 pp. (in Russian)

Weare, E. C., 1994: Interrelationships between cloud properties and sea surface temperatures on seasonal and interannual time scales. *J. Climate*, **7**(2), 248–260.